Appendix

6.1 Quantitative Result Comparison. Fig. 7 and 8 illustrate the quantitative result of ASA, BR, UE, and EV of nine advanced superpixel segmentation algorithms and our SIT-HSS on SBD and PASCAL-S datasets. SIT-HSS demonstrates strong performance in multiple metrics. Its improvement in the ASA metric highlights the algorithm's ability to maintain similarity to the target, particularly notable at high superpixel counts. In contrast, while other algorithms perform well in certain scenarios, they generally fall short compared to SIT-HSS. In terms of the BR and UE metrics, SIT-HSS also excels, effectively capturing target boundaries and reducing under-segmentation errors, thereby enhancing the accuracy of the segmentation results. Regarding the EV metric, SIT-HSS maintains a high level of feature retention capability and exhibits excellent structural consistency, further affirming its advantages in superpixel segmentation tasks.

6.2 Hyperparameter Study. As t and τ vary, we examine the changes in the performance of SIT-HSS on SBD and PASCAL-S datasets. The results are presented in Fig. 9 and 10.

Weight normalization parameter t: The selected values of t are 0.05, 0.10, 0.15, and 0.20. Figs. 9a and 10a indicate that SIT-HSS performs best when $t = 0.1$. Smaller t values result in a decrease in the overall precision of the segmentation, while larger t values lead to less refined boundaries.

Structural entropy threshold τ: The selection of the value τ is based on the characteristics of the datasets and the model sensitivity analysis. For the SBD dataset, where the image complexity is relatively lower, larger thresholds help reduce unnecessary noise. Therefore, we set the values of τ at $1e-6$, $2e-6$, $3e-6$, and $4e-6$. As shown in Fig. 9b, when τ is set to $1e-6$, SIT-HSS performs best on SBD. In contrast, as illustrated in Fig. 10b, when τ is set to $2e-7$, SIT-HSS achieves optimal performance on PASCAL-S. Smaller τ values result in lower boundary adhesion, while larger τ values cause the model to focus too much on the boundaries, resulting in a slight decrease in the consistency of the region and the overall quality of segmentation.

6.3 Convergence Analysis. The proposed algorithm is capable of rapidly converging in a few iterations, achieving accurate superpixel segmentation. To validate this, we randomly select an image from each dataset and record the changes in the number of superpixels and the number of edges between them during each iteration. As shown in Fig. 11, as iterations progress, both the number of superpixels and the number of edges exhibit an exponential decline. On average, by the seventh iteration, the number of superpixels approaches the target segmentation size, and by the 10th to 12th iteration, it precisely reaches the target size of 600. Note that the algorithm's time complexity is linearly related to the number of edges between superpixels. As the number of edges decreases, the computation time required for subsequent iterations also decreases accordingly.

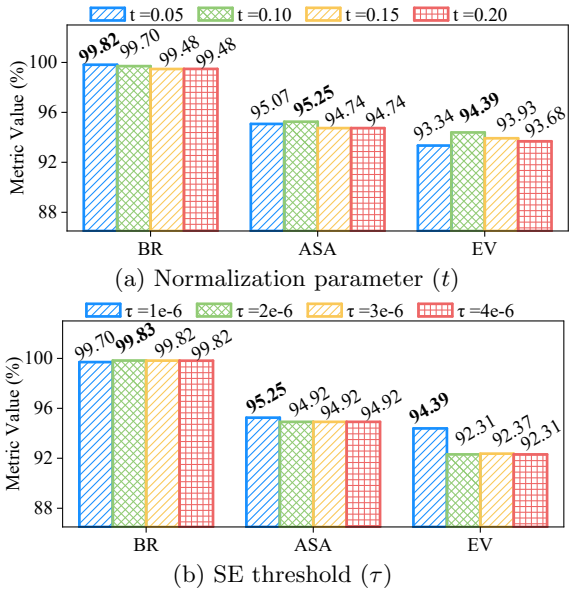

(a) Normalization parameter (t)

(b) SE threshold (τ)

Figure 9: Performance of the SIT-HSS on SBD with different hyperparameter settings.

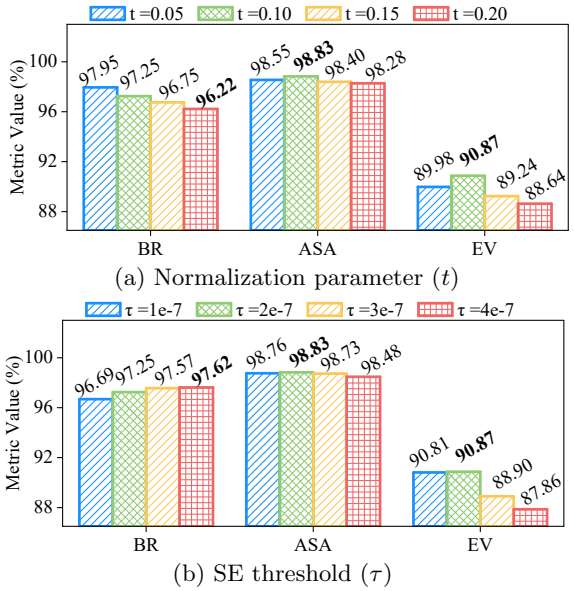

(a) Normalization parameter (t)

(b) SE threshold (τ)

Figure 10: Performance of the SIT-HSS on PASCAL-S with different hyperparameter settings.

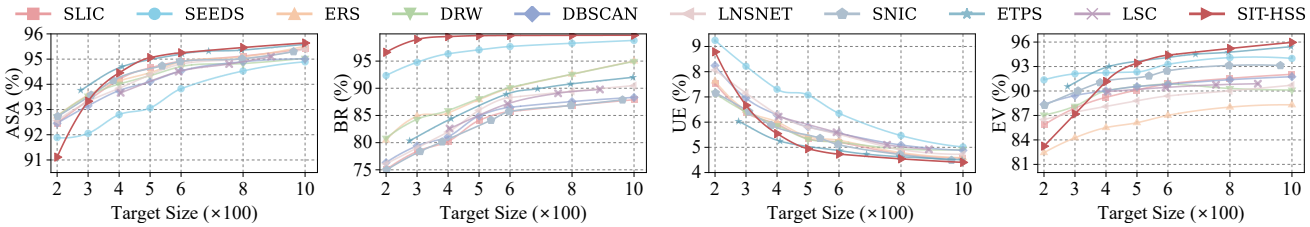

Figure 7: ASA, BR, UE, and EV Curve of our SIT-HSS compared with other state-of-the-art superpixel segmentation algorithms on the SBD dataset.

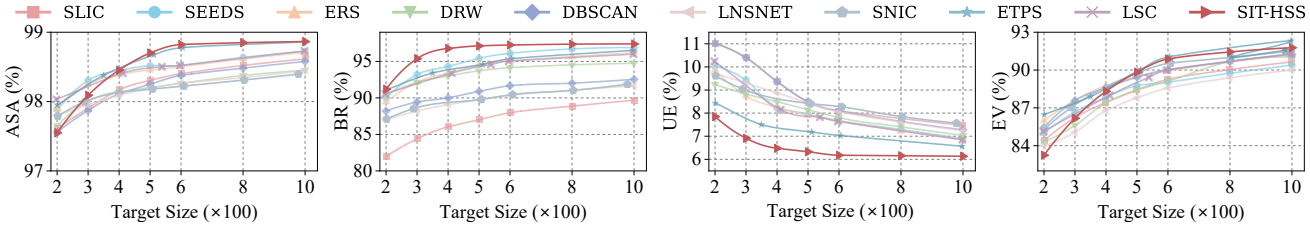

Figure 8: ASA, BR, UE, and EV Curve of our SIT-HSS compared with other state-of-the-art superpixel segmentation algorithms on the PASCAL-S dataset.

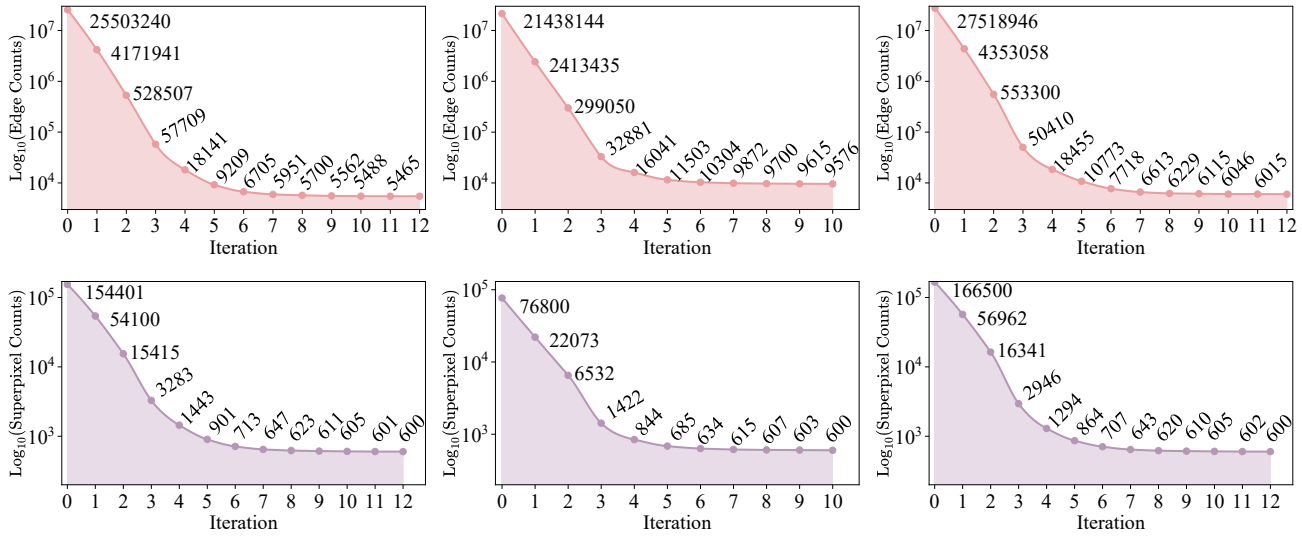

(a) BSDS500 (b) SBD (c) PASCAL-S

Figure 11: The changes in the edges numbers and superpixel numbers between them at each iteration from images in BSDS500, SBD, and PASCAL-S datasets.